Rev. Int. Contam. Ambie. 37, 501-512, 2021
https://doi.org/10.20937/RICA.53820

THERMODYNAMIC AND ELECTROCHEMICAL STUDY OF VANADIUM SOLUTIONS: TOWARDS VANADIUM RECOVERY FROM A SPENT CATALYST

Estudio electroquímico y termodinámico de soluciones de vanadio: hacia su recuperación a partir de un catalizador gastado

Fidel HERNÁNDEZ-PÉREZ, René ANTAÑO-LÓPEZ and Fabricio ESPEJEL-AYALA*

Centro de Investigación y Desarrollo Tecnológico en Electroquímica, Parque Tecnológico Querétaro s/n, 76703 Pedro Escobedo, Querétaro, México.

*Author for correspondence: fespejel@cideteq.mx

(Received: December 2019; accepted: November 2020)

Key words: vanadium, industrial wastes, spent catalyst, electrochemical processes, Pourbaix diagrams, zeolites.

ABSTRACT

Due to the low abundance of vanadium in nature (about 135 g/t), the feasibility to recover it from industrial wastes has highly attracted scientific and technological attention. The main recovery routes reported are associated with chemical or thermochemical processes. However, the electrochemical recovery of vanadium from industrial wastes has been poorly investigated. In this work, a thermodynamic and electrochemical study for the possible vanadium recovery from a spent catalyst generated in the petrochemical industry was conducted. The study was divided into two stages using low vanadium concentrations. In the first stage, the recovery of vanadium was possible in its V^{4+} state at low reduction potentials, whereas for the second stage, cyclic voltammetry was used to calculate the diffusion coefficient and the heterogeneous velocity coefficient of the V^{5+}/V^{4+} redox pair. The obtained values are similar to those reported in the literature for aqueous solutions at high vanadium concentrations and would allow the design of the system at large scale. This report aims to set the conditions for the possible vanadium recovery from a spent catalyst by means of electrochemical processes, although the optimization of such conditions must be further explored.

Palabras clave: vanadio, residuos industriales, catalizador gastado, procesos electroquímicos, diagramas de Pourbaix, zeolitas.

RESUMEN

Debido a la baja abundancia de vanadio en la naturaleza (aproximadamente 135 g/t), es alta la factibilidad científica y tecnológica para recuperarlo a partir de residuos industriales. Las principales formas de recuperación se asocian con procesos químicos y termoquímicos. Sin embargo, la recuperación electroquímica de vanadio a partir de residuos industriales ha sido poco investigada. En este trabajo se realizó el estudio electroquímico y termodinámico para la posible recuperación de vanadio a partir de un catalizador gastado generado en la industria petroquímica. El estudio se dividió en dos etapas empleando bajas concentraciones de vanadio. En la primera etapa, fue posible la recuperación de vanadio en el estado V^{4+} a bajos potenciales de reducción mientras que en la segunda etapa se utilizó la voltametría cíclica para calcular el coeficiente de difusión y el coeficiente de velocidad heterogéneo del par redox V^{5+}/V^{4+}. Los valores obtenidos son similares a lo reportado en la literatura para soluciones acuosas a altas concentraciones de vanadio y permitirían diseñar el sistema a gran escala. Este reporte se centra en fijar las condiciones para la posible recuperación de vanadio a partir de un catalizador gastado por medio de un proceso electroquímico, aunque la optimización de tales condiciones debe ser explorada.

INTRODUCTION

The natural abundance of vanadium (V) is about 135 g/t, occupying the fifth place between the transition metals and 22th in all of the elements in the Earth's crust. Approximately, 80 % of the vanadium production is used to fabricate stainless steel, catalysts, ceramics, and batteries (Imtiaz et al. 2015). Due to the great demand of resources, the extraction and recovery of vanadium from alternative materials as wastes is a feasible strategy. Slags and tailings are the principal wastes used in the recovery of vanadium by hydrometallurgical methods. The oxidation with MnO_2 or using organic solvents to recover vanadium generates wastes; moreover, the selectivity in these processes is not high. In other processes, calcium reduction, thermal decomposition, solvent extraction, and electrolytic refinement are the main steps involved in the recovery of vanadium. Electrolytic refinement with molten salts has the advantage to recover vanadium with high purity. Lei and Sullivan (1971) used an electrolytic bath of LiCl-KCl-VCl_2 at 893 ºK with an efficiency of 73 % for recovering vanadium with Cr, Fe and O at low concentration (200 ppm). Tripathy et al. (2003) proposed another system employing the nitride conversion of V_2O_5, thermal decomposition of nitride and electro-refinement. Using this process, expensive metallic reducers were eliminated obtaining vanadium in concentrations between 98.50 and 99.85 %; however, a high-energy input was necessary. Therefore, new ecofriendly processes for the recovery of vanadium are necessary.

Electrochemical processes provide an alternative for the selectivity in the recovery of vanadium from wastes. However, systematic studies with low vanadium concentration solutions have not been implemented. The electrochemical study of vanadium solutions has been thoroughly investigated due to the interest to understand the complex processes under vanadium redox batteries. Five changes in oxidation states in vanadium solutions have been reported and the thermodynamic potentials have only been determined for concentrated solutions in acid medium. Elouadseri et al. (1986) determined the thermodynamic potential for the redox process in vanadium solutions using carbon paste electrode vs. the saturated calomel electrode (SCE) in 1 M HCl and $NaVO_3$ solution by voltammetry at 60 mV/min. They observed three cathodic and anodic signals at 0.68, 0.39, 0.57 V, and –0.47, +0.28, 0.27 V, respectively, corresponding to the reduction of V^{5+}, V^{4+}, and V^{3+}. Barrado et al. (1997) determined the redox process of vanadium using a carbon paste electrode vs. $Ag|AgCl|KCl|_{sat}$ by voltammetry at 0.5 $mVmin^{-1}$ using HCl as an electrolyte. A charge transfer process occurred between the electrode and the dissolved species displayed fast V^{5+}/V^{4+} and V^{3+}/V^{2+} processes with a low displacement of cathodic and anodic signals. In contrast, the V^{4+}/V^{3+} process is slow, and the reduction signal overlapped with the V^{3+}/V^{2+} signal. On the other hand, Sum and Skyllas-Kazacos (1985) investigated the V^{5+}/V^{4+} and V^{3+}/V^{2+} systems in vanadium redox batteries determining the diffusion coefficient (D) and the heterogeneous velocity constant (k^o) at several concentrations and pH values using a glassy carbon electrode. They showed that the V^{5+}/V^{4+} system has electrochemical reversibility ($k^o = 7.5 \times 10^{-4}$ cm/s; $D = 5.70 \times 10^{-6}$ cm²/s), whereas the V^{3+}/V^{2+} system is irreversible with a $k^o = 1.20 \times 10^{-4}$cm/s.

Several works have developed the technology for the recovery of Cu, Au, Ag, Pb, Zn, and Mn from batteries, computers, cell phones, electronic cards, and mine tailings by hydrometallurgical and electro-reduction processes (Alonso et al. 2004, 2008, Poisot-Díaz et al. 2008, 2012). The results show a clear advantage in the selectivity; however, the principal condition is that the electro-reduction potential must be quite separated. In this work, the results of the thermodynamic and electrochemical study of vanadium solutions (at low concentrations) are presented highlighting the possibility to electrochemically recover vanadium from a spent catalyst generated in the petrochemical industry. The petrochemical industry generates spent catalysts classified as dangerous and their stabilization and adequate disposal are necessary. Catalysts are deactivated due to the catalytic cracking processes where coke and heavy metals are deposited on the catalyst's surface. Worldwide, the generation of spent catalysts in the petrochemical industry oscillates between 150 000-170 000 t/year containing approximately 0.2 % of vanadium (Chiranjeevi et al. 2016). Currently, the recovery processes of this metal from wastes involve adsorption, ion exchange, acid or alkaline leachate and bioleaching (Campbell et al. 1988, Crnojevich et al. 1990, Xiao et al. 2010). In this context, the present work aims to study the thermodynamic and electrochemistry processes in low concentration solutions to determine the potential reduction of vanadium.

EXPERIMENTAL

Materials

Vanadium solutions were prepared using a $NaVO_3$ (Sigma Aldrich) salt at 3.60, 7.20, and 10.80 mM. Vanadium concentrations were chosen considering the total vanadium in the spent catalyst used in this work. H_2SO_4 (J.T. Baker) was used as an electrolyte at 0.50, 1, 3, 5, and 7 M.

Procedure description

The methodology was divided in three stages: (1) sample spent catalyst characterization, (2) thermodynamic study of low concentration of vanadium aqueous solutions, and (3) electrochemical study of vanadium in aqueous solutions. Spent catalyst samples were obtained from the petrochemical plant Antonio Dovalí Jaime in Mexico. Samples were characterized by X-ray diffraction (XRD) and inductively coupled plasm optical emission spectroscopy (ICP-OES).

Thermodynamic studies were conducted by plotting the Pourbaix diagrams of vanadium-water (V-H_2O) and vanadium-sulfur-water (V-S-H_2O) at 25 ºC and 1 atm, calculating the Gibbs energy in all species using the Nernst equation (Pourbaix 1996). Predominance zone (DZP) and species fraction diagrams (SFD) were elaborated using the MEDUSA software which uses an algorithm developed by Eriksson (1979), complemented with HYDRA data that uses stability constants for metal complex from the National Institute of Standards and Technology. DZP and SFD were plotted considering vanadium and sulfate concentrations of 0.000001 and 0.1 M, respectively.

Electrochemical study

Cyclic voltammetry (CV) was performed using a potentiostat/galvanostat Bio-Logic SP-50. The electrochemical cell (25 mm) used a three electrodes configuration, working, reference and counter electrode, glassy carbon, $Ag|AgCl|KCl|_{sat}$ and carbon felt, respectively. CV was implemented at 1, 5, 10, 20, 30, 40, 50, 60, 70, 80, 90 and 100 mV/s in cathodic direction between –0.80 and 1.37 V vs. $Ag|AgCl|KCl|_{sat}$. Different scanning rates were chosen to analyze the heterogeneous electron transfer coefficient (k^o) and the diffusion coefficient (D).

RESULTS AND DISCUSSION

The chemical composition of the spent catalyst is showed in **table I.** The content of vanadium was approximately 0.45 %.

TABLE I. CHEMICAL COMPOSITION OF THE SPENT CATALYST.

Element % (w/w)	Sample 1	Sample 2	Sample 3	Average
Ti	0.42	0.43	0.49	0.45 ± 0.04
V	0.20	0.57	0.58	0.45 ± 0.22
Ni	0.10	0.04	not detected	0.07 ± 0.05
Si	26.82	20.34	17.74	21.63 ± 4.68
Al	11.95	22.87	21.76	18.86 ± 6.01

On the other hand, the XRD result shows the typical pattern of zeolite Y, type faujasite used as an acid catalyst in the cracking process (**Fig. 1-SM** in the supplementary material). Titanium content is in relative proportion to the vanadium concentration while Ni is 6.4 times lower than vanadium. In the case of Ni, the possible electrochemical deposition potential could interfere with the vanadium reduction potential. However, the potential, in which Ni is deposited, is very negative. Gómez et al. (1995) determined the potential reduction of Ni in a Pt electrode at –0.40 V but, using a Ni electrode, where the reduction potential was more negative. Guo et al. (2015) achieved the deposition of Ni over glassy carbon at –1.25 V. For Ti, the electrodeposition occurs in a similar route at very negative potentials using complex agents and basic electrolytes (Rao and Triveti 2005). Gussone et al. (2020) carried out the electrodeposition of Ti in molten salt medium at –0.4 V and 700 ºK indicating that the eletrodeposition of Ti is extremely endothermic and, at room temperature, the electrodeposition is impossible and competitive with the hydrogen evolution.

Thermodynamic study

Pourbaix diagrams were built considering the vanadium species to form V^{5+}, V^{4+}, V^{3+}, and V^{2+}. **Figure 1** indicates the formation of cationic and anionic species at low (< 3) and high pH values (> 3), respectively. Divalent and trivalent species act as cations while, at higher oxidation values, cations and anions are present. Moreover, VOH^+, VO^+, and VOH^{2+} cations appear and polynuclear V_2O_4, V_2O_5, $H_2V_{10}O_{28}{}^{4-}$, $H_2V_{10}O_{28}{}^{5-}$, $V_4O_{12}{}^{4-}$ and $HV_2O_7{}^{3-}$ disappear. **Figure 1b** shows the presence of $VO_2{}^+$ (pentavanadyl cation) in aqueous medium at low pH values (< 3.6) at 10 mM concentration but, when the concentration increases to 1 mM, the pH decreases to 1.3 promoting the formation of V_2O_5 between pH 1.3 and 3.6. Above the electrode potential at the point of zero charge (pH = 1-2) anions are formed, being a disadvantage to stabilize the pentavanadyl ion (Zhou et al. 2011).

Divalent vanadium species are not stable in aqueous medium at 25 ºC in the total interval of pH; in fact, the occurrence of divalent vanadium in nature is less probable (Zhou et al. 2011). Twelve species occur simultaneously classifying them in cationic [$VO_2{}^+$], neutral [$VO(OH)_3$] and anionic. The last ones are divided in decavanadate [$V_{10}O_{26}\,(OH)_2{}^{4-}$, $V_{10}S_{27}(OH)^{5-}$, $V_{10}S_{28}{}^{6-}$] and poly-vanadate species [$VO_2(OH)^{2-}$, $VO_3(OH)^{2-}$, $VO_4{}^{3-}$ y $V_2O_6(OH)^{3-}$, $V_2O_7{}^{4-}$, $V_3O_9{}^{3-}$, $V_4O_{12}{}^{4-}$]. As can be seen in **Figure 1b**, vanadium species in aqueous medium are varied and depend on the vanadium activity. Vanadium ions are mono-molecular at low concentrations in an aqueous medium; as the concentration increases, the mono-molecular species are displaced by poly-vanadate species. The theoretical hydrolysis reaction of vanadium at 0.01 and 0.000001 mM are showed in reactions 1 and 2, respectively (Povar et al. 2019):

$$VO_2{}^+ + 2H_2O = H_2VO_4{}^- + 2H^+ \tag{1}$$

$$10VO_2{}^+ + 8H_2O = H_2V_{10}O_{28}{}^{4-} + 14H^+ \tag{2}$$

Pourbaix diagrams show V^{5+}, V^{4+}, V^{3+}, and V^{2+} species considering the sulfur in the medium (**Fig. 2a**, **b**). Comparing the V-S-H_2O and V-H_2O systems, sulfate substitute hydroxide ions forming several vanadium sulfate species. $HSO_4{}^-$ ions increase the stability of V^{3+}, VO^{2+} and $VO_2{}^+$ promoting the formation of $VSO_4{}^+$, $VOSO_4$ ions while $VO_2SO_4{}^-$ is stable in the pH of 0 to 5. Moreover, the predominant areas increase while vanadium activities decrease. Reduction of $VO_2{}^+$ to VO^{2+} occurs at 1.3 V vs. the normal hydrogen electrode (NHE) (1.12 vs. Ag|AgCl|KCl|$_{sat}$), while the change of VO^{2+} to V^{3+} occurs at 0.25 V vs. NHE. V^{2+} is a thermodynamically unstable reducer agent; however, V^{2+} could be prepared in aqueous medium at higher overpotential values. Therefore, vanadium cannot be reduced to metallic state in aqueous medium. Moreover, considering the presence of Ni in the medium, the standard potential to realize V^{3+} to V^{2+} reduction is close to the Ni^{2+}/Ni reduction (–0.26 V vs. NHE) interfering in the possible recovery of vanadium from the spent catalyst.

In a multi-oxidant system, V-S-H_2O, $VO_2{}^+$, and vanadium act as oxidants and reducers. In this

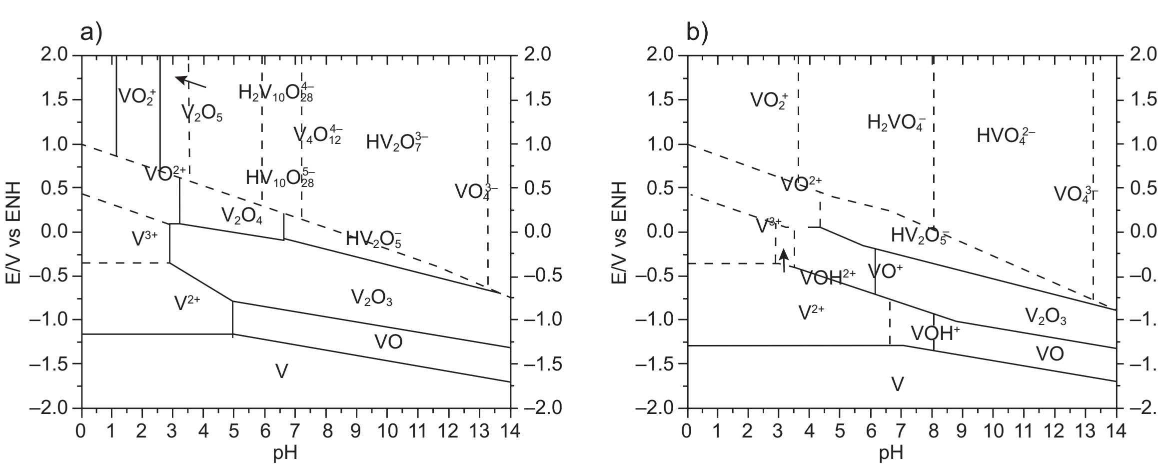

Fig. 1. Pourbaix diagrams for the V-H_2O system with activity of 1 at 25 ºC. Vanadium activity at (a) 0.01 mM and (b) 0.001 mM.

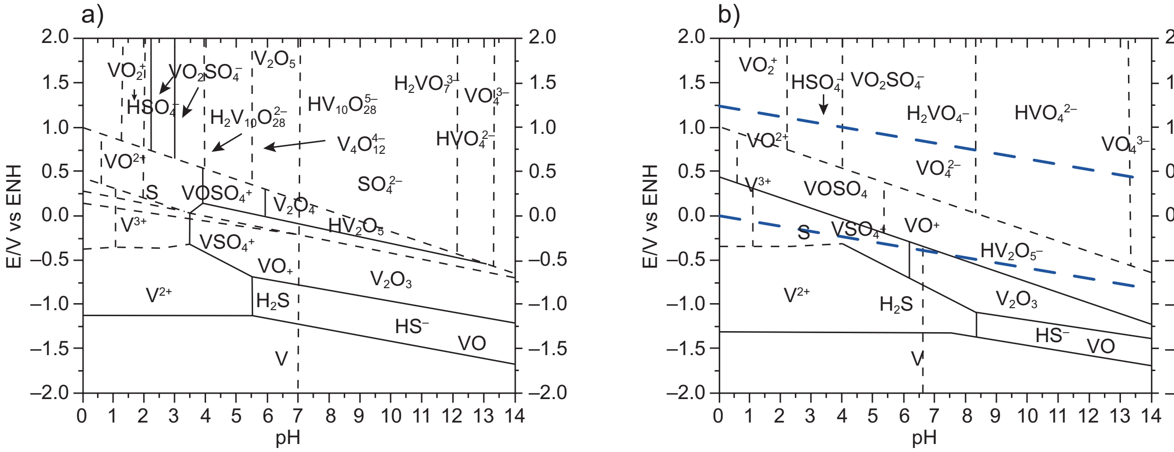

Fig. 2. Pourbaix diagrams for the V-S-H_2O system with S activity of 1 at 25 ºC. Dissolved vanadium activity at (a) 0.01 mM and (b) 0.000001 mM.

case, the VO_2^+/VO^{2+} system is more oxidant in an acid medium and more reducer in alkaline. In fact, the pentavanadyl ion only accepts electrons and vanadium gives up electrons while the intermediate VO^{2+}, V^{3+}, and V^{2+} act simultaneously as oxidants and reducers. In the case of DZP, there are zones with vanadyl sulfate, VO_2SO^{4-} (**Fig. 3a, b**) in a pH between 0 to 5 at higher concentrations of SO_4^- (> 30 mM, $\log[SO_4]^{-2} < 1.5$). Moreover, there are three hydroxides at pH higher than 3: $VO(OH)_3$, $VO_2(OH)_2^-$ and VO_3OH^{2-}.

In the case of 0.01 M of VO^{2+} the predominance interval decreases to 0.5 (**Fig. 3b**). For the system V^{4+}-SO_4^{2-}, VO_2^+ ion predominates a low pH (< 3.5) in a concentration of 1 mM of SO_4^-. When the concentration is 10 M the presence of VO_2^+ at pH = 0.5 is observed (**Fig. 4**).

The vanadium ion (VO_2^+) at low concentration is present in the pH interval of 0 to 5 while, at higher concentration, the pH decreases at 2. The latter promotes vanadium oxides and hydroxides that precipitate at higher pH, although, vanadium is dissolved with the hydrogen evolution in alkaline and acid media (Evans and Garrels 1958). Vanadyl sulfate formation occurs at a low pH of 2.21 and 47 mM. **Figure 5** shows the fraction of V^{5+}, V^{4+}, and V^{3+} species. The pentavanadyl fraction decreases as pH increases; moreover, vanadyl sulfate and hydroxide

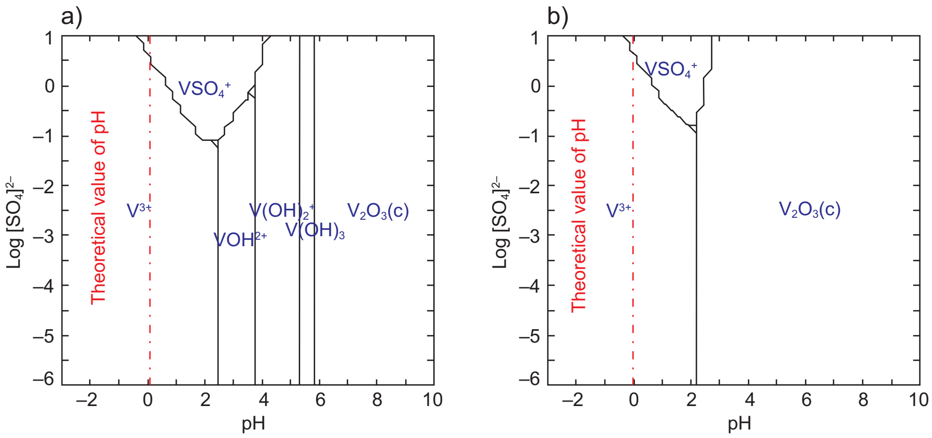

Fig. 3. Predominance zone diagram of species for the VO^{2+}-SO_4^{2-} system at pH = 0-10. Vanadium concentrations of (a) 0.001 mM and (b) 10 mM. $\log[SO_4]^{-2}$ = 0.001 and 10 M at 298.15 ºK and 1 atm.

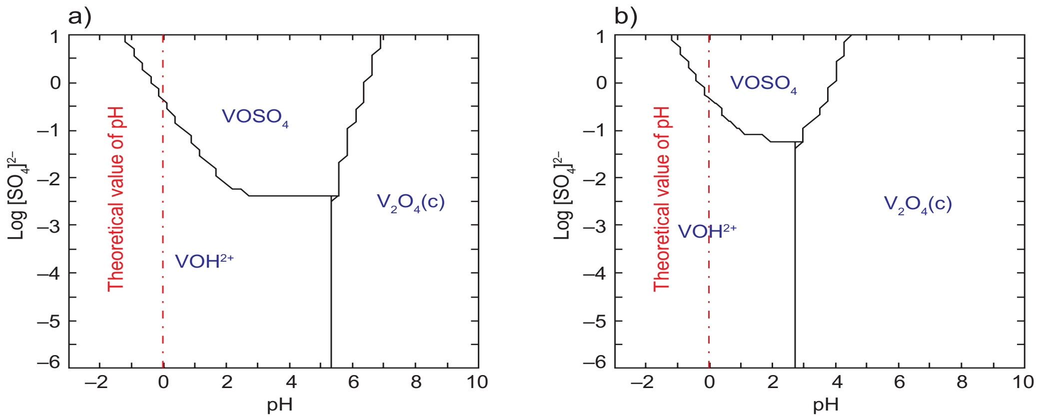

Fig. 4. Predominance zone diagram of species in the VO^{2+}-SO_4^{2-} system at pH –3 to 10 and sulfate concentration of 0.001 to 10 M at 298.15 ºK and 1 atm. Vanadium concentrations of (a) 0.001 mM and (b) 10 mM.

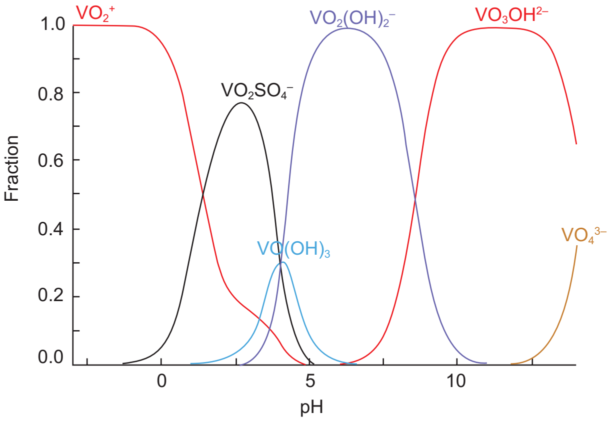

Fig. 5. Fraction species diagram of V^{5+}, V^{4+} and V^{3+} ions at 298.15 ºK and 1 atm.

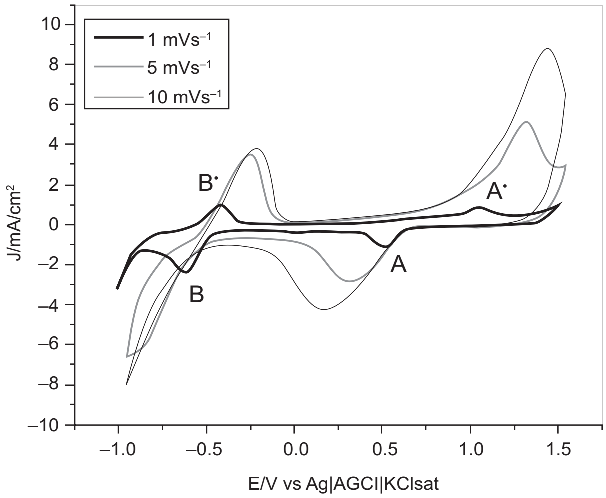

Fig. 6. Cyclic voltammogram for 3.6 mM $NaVO_3$ + 0.5 M H_2SO_4 using carbon felt as working electrode.

species as $VO(OH)_3$, $VO(OH)_2^-$, VO_3OH^{2-} and VO_4^{3-} appear as the pH becomes more alkaline.

When the H_2SO_4 concentration increases, the total concentration of sulfate ion surpasses the equilibrium and leads to the decrease of vanadium sulfate species. Rahman and Skyllas-Kazacos, (2009) determined that the V^{5+} ion is more stable even at high concentrations of sulfate and bisulfate (3 and 6 M); however, the behavior in real solutions could be different due to the possible Ni and Ti lixiviation from the spent catalyst. Nevertheless, an acid medium was chosen to study the electrochemistry process for vanadium recovery from a spent catalyst.

Electrochemical study

To investigate the electrochemical behavior of vanadium solutions, cyclic voltammetry was performed at different conditions. **Figure 6** shows the cyclic voltammogram for the 3.6 mM $NaVO_3$ solution and 0.5 M H_2SO_4 using carbon felt as a working electrode measured at 1, 5 and 10 mV/s. Those scan velocities were chosen to show the redox process since at high scan velocities vanadium signals were not observed. The carbon felt did not undergo a previous treatment; it was only wetted during a short time to release the oxygen present on the surface.

A and A' correspond to the V^{5+}/V^{4+} pair whereas B and B' to the V^{3+}/V^{2+} pair. Potential values are in agreement with those reported by Pour et al. (2015), who recorded the reduction and oxidation potential at –0.5 V vs. SCE attributed to the V^{3+}/V^{2+} pair in a similar concentration to the evaluated in this study. They also observed that the signals are independent of the type of electrolyte, which means the potentials are the same even though the vanadium salt could be different. By using cyclic voltammetry, the chemical irreversibility was calculated for the V^{5+}/V^{4+} process using the criteria of distance between cathodic and anodic peaks. **Table II** shows the scan rate, potential, and distance between signals.

TABLE II. SCAN RATE, POTENTIAL AND DISTANCE BETWEEN THE REDOX SIGNALS STUDIED BY CYCLIC VOLTAMMETRY

V (mV/s)	E_{pc} (V)	E_{pa} (V)	ΔEp (V)
1	A = 0.50 B = 0.61	A ’= 1.05 B’ = –0.42	0.55 1.03
5	A = 0.33 B covered up	A’ = 1.31 B’ = –0.25	0.98
10	A = 0.17 B covered up	A’ = 1.44 B’ = –0.20	1.27

The distance between signals at 1 mV/s was 0.548 V (> 0.6 V) while for 5 and 10 mV/s the distance showed a lineal increase that indicates the electrochemical reversibility of the process. In the case of V^{3+}/V^{2+} only the signals at 1 mV/s were appreciated showing a distance of 0.198 V between peaks. The reduction started at –0.5 V in agreement with the hydrogen evolution that was observed at 5 and 10 mV/s. In order to compare the obtained results a glassy carbon electrode was used as working electrode in a second series of experiments, since this electrode is non-porous and its preparation is not complex. Fifteen cycles were achieved in a potential of –0.8 to 1 V in 3.6 mV $NaVO_3$ + 0.5 M H_2SO_4 at 1 mV/s. **Figure 7** shows the cyclic voltammogram obtained under these conditions.

In **figure 7** six signals are observed with a slight deviation in the potential values with respect to **figure 6**; however, the redox processes V^{5+}/V^{4+} and V^{3+}/V^{2+} appeared at 0.99 and –0.59 V, respectively. The reduction potentials are in line with the study of Elouadseri et al. (1986), who reported potentials of 0.68 and –0.57 V vs. SCE.

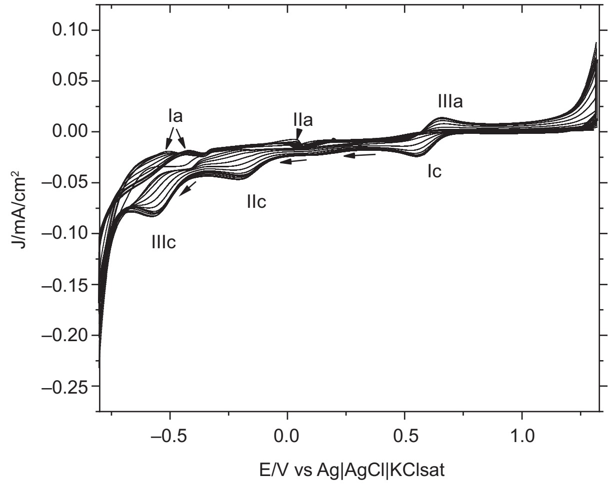

Fig. 7. Cyclic voltammogram obtained using glassy carbon electrode and 3.6 mV $NaVO_3$ + 0.5 M H_2SO_4 at 1 mV/s.

When the concentration of the supported electrolyte increased to 7 M, the value of the reduction signals remained the same. Electrolyte concentrations were increased to verify voltammetry signals; however, a low concentration is preferable in order to decrease costs and avoid contaminant effluents. Although the three processes were studied, the V^{5+}/V^{4+} reduction was the most interesting for this study, because the first reduced state would allow the recovery of vanadium from the spent catalysis; moreover, when the potential is more negative, the provided energy in the reaction could increase the total cost of the process (**Fig. 8**). Considering that this process is reversible, the diffusion coefficients were estimated using equation 3:

$$i_p = 2.69 \times 10^5\, n^{3/2} A C^* D^{1/2} v^{1/2} \qquad (3)$$

where I_p is the cathodic current in amperes, n is the number of transferred electrons in the electrochemical reaction, A is the area of the electrode in cm^2,

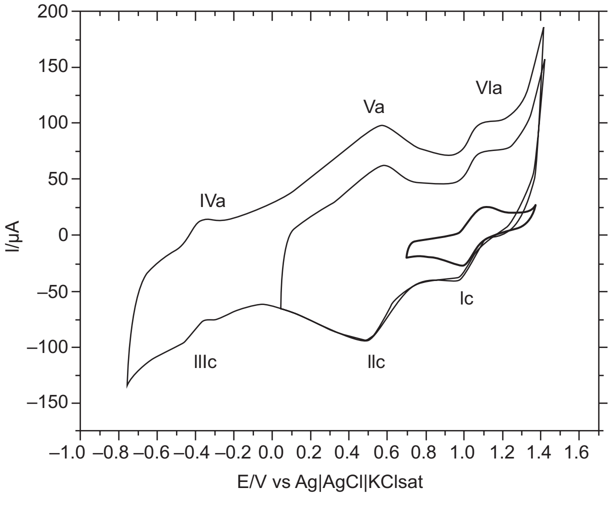

Fig. 8. Cyclic voltammogram obtained using the glassy carbon electrode and 7.2 mM $NaVO_3$ + 5 M H_2SO_4 at 1 mV/s.

C is the concentration of the solution in mol/cm^3, *D* is the diffusion coefficient in cm^2/s, *v* is the scan rate in V/s, and *α* is the charge transfer coefficient. The information obtained in the present study with concentrations of 3.6, 7.2, and 10.8 mM $NaVO_3$ + 7 M H_2SO_4 can be found in the supplementary material (**Fig. SM-2**). **Table III** shows the average values of *D* obtained in this study.

TABLE III. AVERAGE VALUES OF THE DIFFUSION COEFFICIENT (*D*) OBTAINED IN THIS STUDY

Concentration (mM)	*D* (cm^2/s × 10^{-6})
3.60	1.14
7.20	1.20
10.80	1.44

Sum and Skyllas-Kazacos (1985) estimated the diffusion coefficient in the V-H_2SO_4-H_2O system *D* at around 1.40 × 10^{-6} cm^2/s, which is in line with the values reported in this study (**Table I**). These authors also pointed out the importance of the correct selection of *α* in the 0.5 charge transfer coefficient; however, this value is not entirely correct because *α* is associated with the reversibility of the electrochemical reaction. For this reason, the adequate selection of *α* is of vital importance to decrease the estimation error of *D*. This selection is very important because the diffusion is the only mechanism of mass transport involved in this electrochemical process to recovery vanadium. Although convection or migration are present in an electrochemical reactor, their contribution can be neglected. Moreover, CV allows to estimate the presence of coupled reactions or other processes that could affect the redox pair V^{5+}/V^{4+}.

To estimate the presence of coupled reactions, the relations i_{pc} vs. $v^{1/2}$ and $i_{pc}/v^{1/2}$ vs. v were analyzed. **Figure SM-3** of the supplementary material shows the lineal dependence between the cathodic current signals and the scan rate, which is observed at two concentrations of vanadium. However, the $v^{1/2}$ vs. i_{pc} relation does not show a constant behavior due to coupled reactions or processes such as adsorption, double layer charge, or contributions by convection. In the case of the 10.8 mM concentration (**Fig. SM-3**), $v^{1/2}/i_{pc}$ decreases while the scan rate increases, showing a similar behavior as in Barrado et al. (1997), although the scan velocities were different (0.1, 0.5, 1.0 and 2.0 mV/s). These authors suggested the following irreversible reaction:

$$NaVO_3\ (s) + 2H_3O^+ \rightarrow Na^+ + VO_2^+ + 3H_2O \qquad (4)$$

Afterwards, an electrochemical reduction occurs as follows:

$$VO2^+ + 2H_3O^+ + 1e^- \rightarrow VO^{2+} + 3H_2O \qquad (5)$$

The heterogeneous velocity constants k^o were calculated for the different concentrations of vanadium evaluated in this work. In general, k^o represents the kinetic facility for a redox pair to occur, and it was calculated using equation 6 in its lineal form:

$$i_p = 0.227\ nF\ C_O^O\ k^O \exp\left[-\frac{(\alpha nF)}{(RT)}\ (E_p - E^{0\prime})\right. \qquad (6)$$

An ln(i_p) vs. (E_p-$E^{o\prime}$) chart was elaborated at several scan rates with a slope of (-αnF/RT) and an interception in k^o. The formal electrode potential $E^{o\prime}$

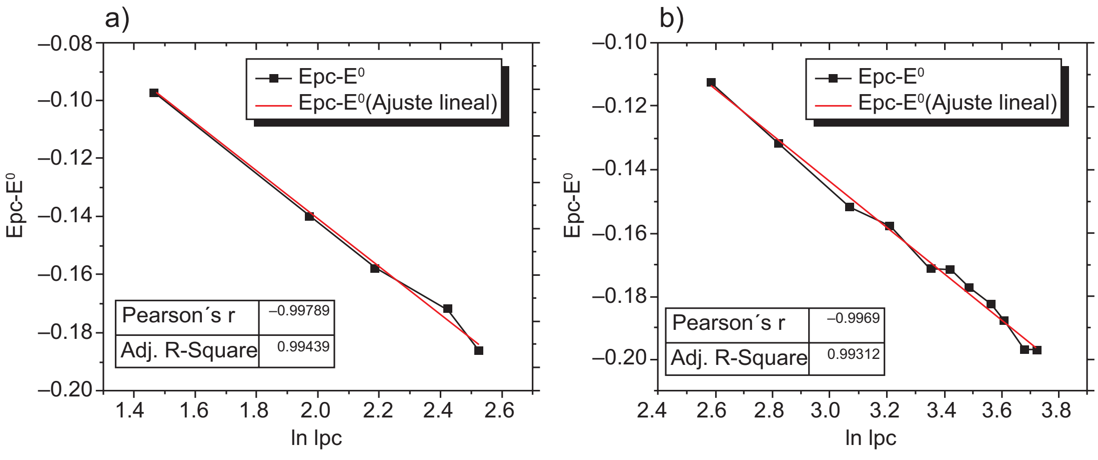

Fig. 9. Ln(i_p) vs. (E_p-$E^{o\prime}$) chart of (a) 7.2 mM $NaVO_3$ + 7 M H_2SO_4 and (b) 10.8 mM $NaVO_3$ + 7 M H_2SO_4.

was calculated from cyclic voltammograms considering the average in the anodic and cathodic potentials, E_{pa} and E_{pc}, respectively (equation 7):

$$E^{0\prime} = \frac{\sum_{i=1}^{m} (E_{pa_i} + E_{pc_i} / 2)}{m} \tag{7}$$

From the intersection of the right line (**Fig. 9a**), k^{o} was 8.92×10^{-5} cm/s when the concentration of vanadium was 7.2 mM. For a concentration of 10.8 mM of vanadium, k^{o} was estimated around 5.93×10^{-8} cm/s (**Fig. 9b**).

CONCLUSIONS

The possibility of vanadium recovery from a spent catalyst generated in the petrochemical industry by means of electrochemical processes was demonstrated in this report. The thermodynamic study showed the energetic threshold to achieve the reduction of V^{5+} to V^{2+}, even in several steps and in an alkaline medium at low vanadium concentration. The electrochemical study showed the possibility of recovering vanadium at low concentrations in an acid medium. Moreover, the redox pair studies showed an irreversible electrochemical behavior in all of the cases, being the V^{5+}/V^{4+} pair the most interesting for the recovery of vanadium from the spent catalyst. The consumption of H_2SO_4 employed in the electrochemical system to recover vanadium or the inclusion of other organic acids must be considered to make the process more environmentally friendly.

ACKNOWLEDGMENTS

F. Hernández-Pérez thanks CONACYT for his master scholarship. The authors thank SENER-CONACYT for financial support through Grant 247006.

REFERENCES

Alonso A.R., Lapidus G.T. and González I. (2004). A strategy to determine the potential interval for selective silver electrodeposition from ammoniacal thiosulfate solutions. Hydrometallurgy 85, 144-153. https://doi.org/10.1016/j.hydromet.2006.08.009

Alonso A.R., Lapidus G.T. and González I. (2008). Selective silver electrodeposition from ammoniacal thiosulfate leaching solutions using a rotating cylinder electrode reactor (RCE). Hydrometallurgy 92, 115-123. https://doi.org/10.1016/j.hydromet.2008.02.001

Barrado E., Pardo R., Catrillejo Y. and Vega M. (1997). Electrochemical behavior of vanadium compounds at a carbon paste electrode. J. Electroanal. Chem. 427, 35-42. https://doi.org/10.1016/S0022-0728(96)05041-3

Campbell C.A., Peet M. and Ward N.I. (1988). Vanadium and other trace elements in patients taking lithium. Biol. Psychiat. 24, 775-781. https://doi.org/10.1016/0006-3223(88)90253-3

Chiranjeevi T., Pragya R., Gupta S., Gokak D.T. and Bhargava S. (2016). Minimization of waste spent catalyst in refineries. Procedia Environ. Sci. 35, 610-617. https://doi: 10.1016/j.proenv.2016.07.047

Crnojevich R., Wiewirowski E., Tinnin L.R. and Case A. (1990). Recycling chromium-aluminum wastes from aluminum finishing operations. JOM-J. Min. Met. Mat. S. 42, 42-45. https://doi.org/10.1007/BF03220413

Elouadseri M.M., Vittori O. and Durand B. (1986). Reactivite electrochimique de quelques oxydes de vanadium en milieu HCl 1M. Electrochim. Acta 31, 1335-1339. https://doi.org/10.1016/0013-4686(86)80157-8

Eriksson G. (1979). An algorithm for the computation of aqueous multi-component, multiphase equilibria. Anal. Chim. Acta 112, 375-383. https://doi.org/10.1016/S0003-2670(01)85035-2

Evans H.T. and Garrels R.M. (1958). Thermodynamic equilibria of vanadium in aqueous systems as applied to the interpretation of the Colorado Plateau ore deposits. Geochim. Cosmochim. Ac. 15, 131-149. https://doi.org/10.1016/0016-7037(58)90015-2

Gómez E., Pollina R. and Valles E. (1995). Nickel electrodeposition on different metallic substrates. J. Electroanal. Chem. 386, 45-56. https://doi.org/10.1016/0022-0728(95)03817-Z

Guo H., Huang Z., Zheng Y. and Weng S. (2015). Electrodeposition of nickel nanoparticles modified glassy carbon electrode for non-enzymatic glucose biosensing. Int. J. Electrochem. Sc. 10, 10703-10712. https://doi.org/10.1002/elan.201200479

Gussone J., Yerragudil Vijay C.R., Watermeyer P., Milicevic K., Friedrich B. and Haubrich J. (2020). Electrodeposition of titanium-vanadium alloys from chloride-based molten salts: influence of electrolyte chemistry and deposition potential on composition, morphology and microstructure. J. Appl. Electrochem. 50, 355-366. https://doi.org/10.1007/s10800-019-01385-0

Imtiaz M., Shahid-Rizwan M., Xiong S., Li H., Ashraf M., Shahzad S.M., Shahzad M., Rizan M. and Tu S. (2015). Vanadium, recent advancements and research prospects: A review. Environ. Int. 80, 79-88. https://doi.org/10.1016/j.envint.2015.03.018

Lei K.P.V. and Sullivan T.A. (1971). Electrorefining of vanadium prepared by carbothermic reduction of V_2O_5. Metall. Mater. Trans. A 2, 2312-2314. https://doi.org/10.1007/BF02917579

Poisot Díaz M.E., Alonso A.R., González I. and Lapidus G.T. (2012). Influence of oxygen reduction and hydrogen evolution in the gold and silver direct electrodeposition process from thiourea in a filter press type reactor. Hydrometallurgy 129-130, 90-96. https://doi.org/10.1016/j.hydromet.2012.09.006

Poisot-Díaz M.E., González I. and Lapidus G.T. (2008). Electrodeposition of a silver-gold alloy (DORÉ) from thiourea solutions in the presence of other metallic ion impurities. Hydrometallurgy 93, 23-29. https://doi.org/10.1016/j.hydromet.2008.02.015

Pour N., Kwabi D.G., Carney T., Darling R.M., Perry M.L. and Shao-Horn Y. (2015). Influence of edge-and basal-plane sites on the vanadium redox kinetics for flow batteries. J. Physic. Chemi. 119, 5311-5318. https://doi.org/10.1021/jp5116806

Pourbaix M. (1996). Atlas of electrochemical equilibria in aqueous solutions. Pergamon, Oxford, 648 pp.

Povar I., Spinu O., Zinicovscaia I., Pintilie B. and Ubaldini S. (2019). Revised Pourbaix diagrams for the vanadium-water system. J. Electrochem. Sci. Eng. 9 (2), 75-84. https://doi.org/10.5599/jese.620

Rahman F. and Skyllas-Kazacos M. (2009). Vanadium redox battery: Positive half-cell electrolyte studies. J. Power Sources 189, 1212-1219. https://doi.org/10.1016/j.jpowsour.2008.12.113

Rao C.R.K. and Triveti D.C. (2005). Chemical and electrochemical depositions of platinum group metals and their applications. Coordin. Chem. Rev. 249, 613-631. https://doi.org/10.1016/j.ccr.2004.08.015

Sum E. and Skyllas-Kazacos M. (1985). A study of the V(II)/V(III) redox couple for redox flow cell applications. J. Power Sources 15, 179-190. https://doi.org/10.1016/0378-7753(85)80071-9

Tripathy P.K., Rakhasia R.H., Hubli R.C. and Suri A.K. (2003). Electrorefining of carbothermic and carbonitrothermic vanadium: A comparative study. Mater. Res. Bull. 38, 1175-1182. https://doi.org/10.1016/S0025-5408(03)00107-7

Xiao Q., Chen Y., Gao Y., Xu H. and Zhang Y. (2010). Leaching of silica from vanadium-bearing steel slag in sodium hydroxide solutions. Hydrometallurgy 104, 216-221. https://doi.org/10.1016/j.hydromet.2010.06.007

Zhou X., Wei C., Li M., Qiu S. And Li X. (2011). Thermodynamics of vanadium-sulfur-water systems at 298 K. Hydrometarllurgy 106, 104-112. https://doi.org/10.1016/j.hydromet.2010.12.003

SUPPLEMENTARY MATERIAL

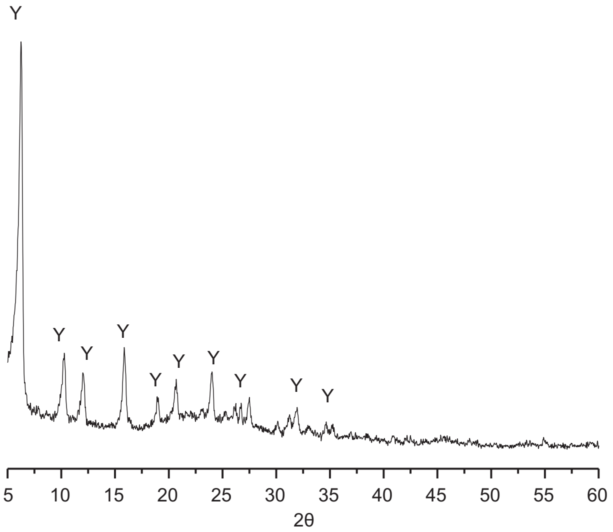

Fig. SM-1. X-ray diffraction pattern of the spent catalyst. Y: zeolite Y (faujasite type).

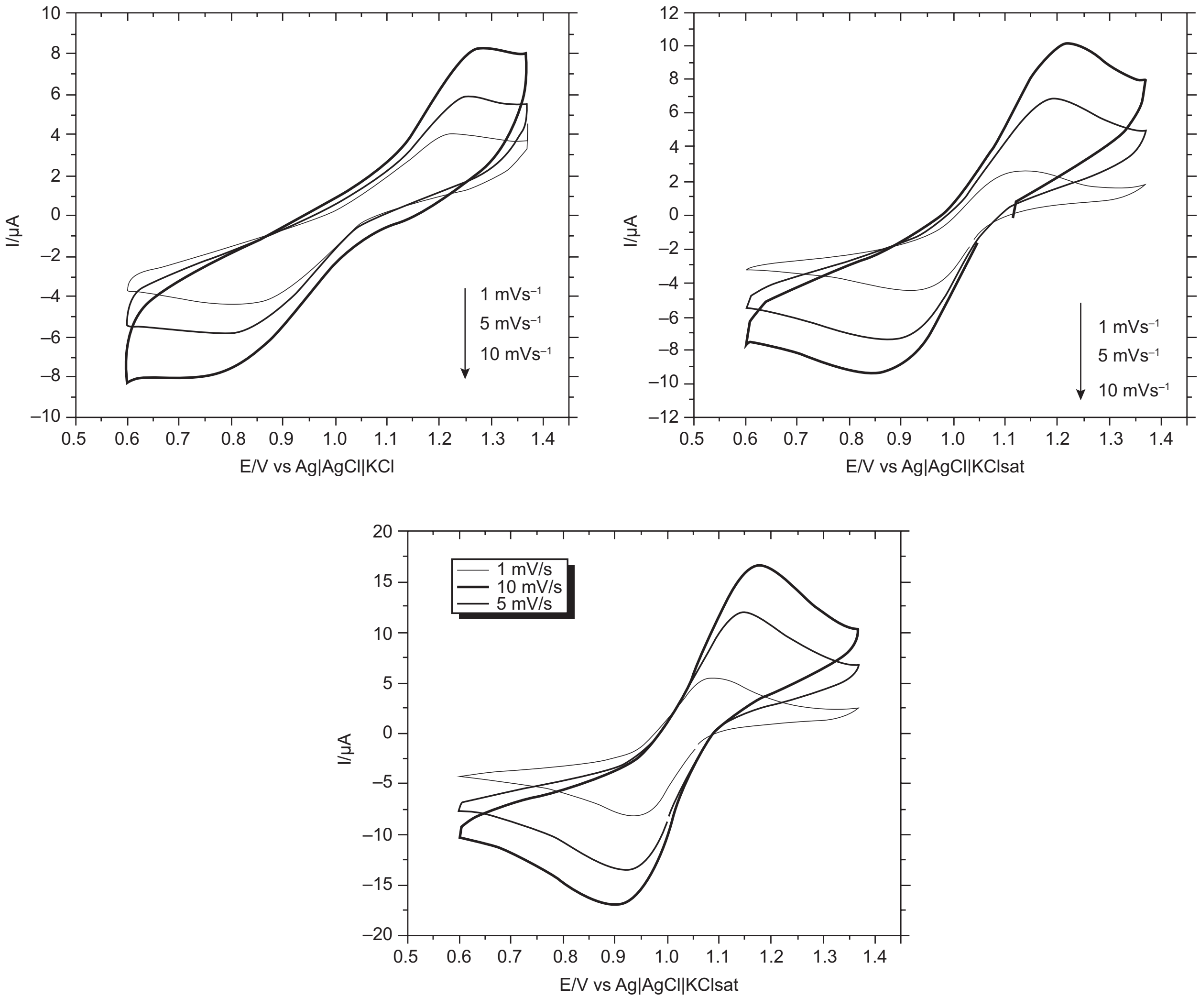

Fig. SM-2. Cyclic voltammogram obtained using the glassy carbon electrode and 3.6, 7.2 and 10.8 mM $NaVO_3$ + 7M H_2SO_4 at 1 mVs^{-1}.

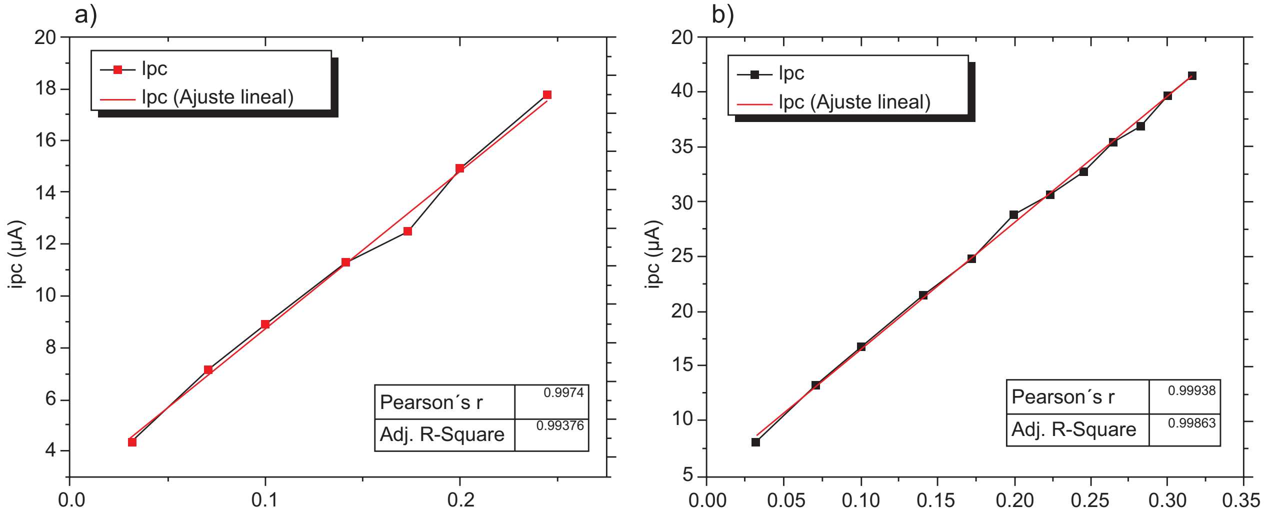

Fig. SM-3. I_{pc} vs. $v^{1/2}$ and $I_{pc}/v^{1/2}$ vs. v relations for (a) 7.2 mM $NaVO^{3+}$ 7 M H_2SO_4 and (b) 10.8 mM $NaVO^{3+}$ 7 M H_2SO_4 in the redox pair V^{5+}/V^{4+}